Anal. Chem. **2004,** *76,* 351−356

Surface-Induced Dissociation of Ions Produced by Matrix-Assisted Laser Desorption/Ionization in a Fourier Transform Ion Cyclotron Resonance Mass Spectrometer

Julia Laskin,* Kenneth M. Beck, John J. Hache, and Jean H. Futrell

Fundamental Science Directorate, Pacific Northwest National Laboratory, P.O. Box 999 (K8-88), Richland, Washington 99352

Intermediate pressure matrix-assisted laser desorption/ionization (MALDI) source was constructed and interfaced with a 6-T Fourier transform ion cyclotron resonance mass spectrometer (FT-ICR MS) specially configured for surface-induced dissociation (SID) studies. First MALDI−SID results in FT-ICR are presented, demonstrating unique advantages of SID over conventional FT-ICR MS ion activation techniques for structural characterization of singly protonated peptide ions. Specifically, we demonstrate that SID on a diamond surface results in a significantly better sequence coverage for singly protonated peptides than SORI-CID. A combination of two effects contributes to the improved sequence coverage: shattering of peptide ions on surfaces opens up a variety of dissociation channels at collision energies above 40 eV, and second, wide internal energy distribution deposited by collision with a stiff diamond surface provides an efficient mixing between the primary reaction channels that are dominant at low internal energies and extensive fragmentation at high internal excitation that results from shattering. Activation of MALDI-generated ions by collisions with surfaces in FT-ICR MS is a new powerful method for characterization and identification of biomolecules

Large molecules can be introduced into the gas phase using soft ionization techniques such as electrospray (ESI)[1] or matrix-assisted laser desorption/ionization (MALDI)[2] and mass-analyzed using a variety of mass spectrometric approaches.[3] Although accurate mass measurement is an important prerequisite for mass spectrometric analysis of peptides and proteins—the focus of proteomics—it is not sufficient for unambiguous identification of these large molecules. For this reason, tandem mass spectrometry, based on structure-specific fragmentation of gas-phase ions, is a critical step for peptide and protein sequencing and identification.[4] Because of the soft nature of ESI and MALDI, fragmentation of ions produced using these techniques requires a separate ion activation step, in which the internal energy of the ion is increased by collisions with a neutral gas or with a surface, multiphoton absorption, or electron attachment.

It is well established that dissociation of gas-phase peptides and proteins is a strong function of their charge state.[5−7] For example, the most reliable structural information for tryptic peptides is obtained from dissociation of doubly protonated ions.[4] Tryptic digestion typically produces peptides with C-terminal arginine or lysine—the most basic amino acids that can sequester a proton. In many cases, fragmentation of singly protonated lysine- and arginine-containing peptides is very specific and provides poor sequence information.[8,9] In most cases, addition of a second proton results in nonspecific fragmentation offering better sequence coverage.[10] Multiply protonated peptide ions are preferentially produced using ESI while MALDI predominantly yields singly protonated species. It is therefore advantageous to use ESI for peptide sequencing. However, MALDI offers unique advantages over ESI, being more robust against sample contamination and providing simpler mass spectra (containing mainly a single charge state) for complex mixtures.

Combination of MALDI with Fourier transform ion cyclotron resonance mass spectrometry (FT-ICR MS) offers very high mass resolution and mass accuracy as well as multiple stages of tandem mass spectrometry (MS^n) that are essential for many applications.[11] However, poor fragmentation patterns commonly obtained for MALDI ions using conventional ion activation techniques in FT-ICR MS such as sustained off-resonance irradiation (SORI-CID) or infrared multiphoton dissociation limit the utility of this combination for structural characterization of biomolecules. In this work, we evaluate the utility of surface-induced dissociation

* Corresponding author. E-mail: Julia.Laskin@pnl.gov. Fax: (509) 3763650.

(1) Fenn, J. B.; Mann, M.; Meng, C. K.; Wong, S. F.; Whitehouse, C. M. *Science* **1989**, *246*, 64.
(2) Hillenkamp, F.; Karas, M.; Beavis, R. C.; Chait, B. T. *Anal. Chem.* **1991**, *63*, 1193A.
(3) McLuckey, S. A.; Wells, J. M. *Chem. Rev.* **2001**, *101*, 571.
(4) Aebersold, R.; Goodlett, D. R. *Chem. Rev.* **2001**, *101*, 269.
(5) Downard, K. M.; Biemann, K. *J. Am. Soc. Mass Spectrom.* **1994**, *5*, 966.
(6) Tang, X.-J.; Thibault, P.; Boyd, R. K. *Anal. Chem.* **1993**, *65*, 2824.
(7) Reid, G. E.; Wu, J.; Chrisman, P. A.; Wells, J. M.; McLuckey, S. A. *Anal. Chem.* **2001**, *73*, 3274.
(8) Cox, K. A.; Gaskell, S. J.; Morris, M.; Whiting, A. *J. Am. Soc. Mass Spectrom.* **1996**, *7*, 522.
(9) Qin, J.; Chait, B. T. *Int. J. Mass Spectrom.* **1999**, *190*/*191*, 313.
(10) Tsaprailis, G.; Nair, H.; Somogyi, A.; Wysocki, V. H.; Zhong, W.; Futrell, J. H.; Summerfield, S. G.; Gaskell, S. J. *J. Am. Chem. Soc.* **1999**, 121, 5142.
(11) Dienes, T.; Pastor, S. J.; Schurch, S.; Scott, J. R.; Yao, J.; Cui, S.; Wilkins, C. L. *Mass Spectrom. Rev.* **1996**, *15*, 163.

10.1021/ac0351116 CCC: $27.50
Published on Web 12/05/2003

(SID)[12,13] for sequencing of MALDI-generated peptide ions. We demonstrate that SID is a valuable alternative to slow activation of MALDI ions in FT-ICR MS that offers significantly better sequence coverage than conventional methods. MALDI and SID have been previously combined with a time-of-flight (TOF) mass spectrometer by Russell and co-workers.[14] FT-ICR SID of ions generated using MALDI and trapped in the ICR cell prior to the activation event was reported by Wilkins and co-workers.[15] McLafferty and co-workers used a similar strategy to dissociate multiply protonated proteins.[16] However, in that study, SID fragments were detected with low efficiency and low-quality MS/MS spectra were obtained. A different approach for conducting SID in FT-ICR MS has been developed in our group, in which externally produced ions are impacted on a surface while the ICR cell is used for collection and mass analysis of resulting fragments.[17,18] This approach has been extensively utilized to study dissociation of ions produced by electrospray ionization.[19] Here we report the first results from combining MALDI and SID of externally generated ions with FT-ICR MS, which has several distinct advantages over TOF instruments for peptide identification. In particular, long reaction time offered by FT-ICR MS enables the observation of primary fragments even for fairly large precursor ions.[19] In addition, high mass resolving power of FT-ICR and multiple MS/MS stages are important for unambiguous identification of fragment ions.

Our detailed studies of the kinetics and dynamics of SID of singly protonated ions (generated using ESI) in FT-ICR MS revealed that at low collision energies ion activation by collisions with surfaces closely mimics multiple-collision activation in the gas phase.[19,20] A clear indication for this finding is the striking similarity between SORI-CID and low-energy SID spectra obtained for both small[20,21] and large peptides.[19] At high collision energies, we observed a transition in the dynamics of ion−surface interaction attributed to instantaneous dissociation of ions on the surface—the shattering transition. Shattering results in opening up a variety of dissociation pathways that cannot be achieved by slow activation methods.[22] The shattering transition is particularly pronounced for arginine-containing peptides that fragment selectively at low collision energies. For example, the low-energy SID spectrum of singly protonated des-Arg^1-bradykinin (PPGFSPFR) contains only two primary fragments: $MH^+ - H_2O$ and y_6 ions. However, at high collision energies, the number of fragment ions undergoes a dramatic increase to 40−50 features in each spectrum.

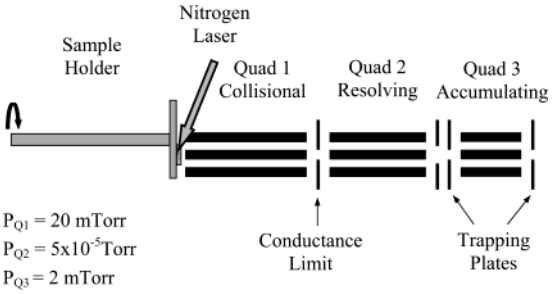

Figure 1. Schematic view of the intermediate-pressure MALDI source.

Despite the very sharp transition from recoil to shattering, high-energy SID spectra commonly contain both primary and high-energy fragments (slow and fast fragmentation). The extent of "mixing" between the slow and fast fragmentation is a function of the width of the internal energy distribution of excited ions. We have recently shown that collisions of peptide ions with soft surfaces such as self-assembled monolayers of alkylthiols on gold results in deposition of relatively narrow, quasi-thermal distributions of internal energies. Substantially wider distributions are obtained by colliding ions with stiff surfaces such as thin films of diamond or lithium fluoride on metal substrates.[23] It follows that stiff surfaces provide a better mixing between the slow and fast fragmentation, presenting a clear analytical advantage for peptide sequencing.

In this work, we present details on the design and performance of a new intermediate-pressure MALDI source[24−26] that enables mass selection and external accumulation of ions prior to their introduction into the ICR cell. First results on the SID using a diamond surface of MALDI-generated ions in FT-ICR MS will be presented, demonstrating a unique analytical utility of SID for sequencing of peptide ions that produce poor fragmentation patterns using conventional ion activation techniques.

EXPERIMENTAL SECTION.

A specially designed 6-T FT-ICR mass spectrometer employed in this work was described in detail elsewhere.[27] The home-built MALDI source is based on the design suggested by Baykut et al.[24] and O'Connor et al.[25,26] The principal scheme of the source is shown in Figure 1. The MALDI target with 10 sample spots is held by a small magnet on a standard Bruker target holder described elsewhere.[24] The sample holder has been modified to enable electrical insulation of the sample plate from the sample holder kept at ground potential. This allows us to apply a desired potential to the sample plate. The sample is placed 1 mm away from a collisional quadrupole (CQ). The axis of the sample holder is displaced from the axis of the CQ in such a way that a sample spot is located exactly on the CQ axis. As a result, switching between different sample spots is achieved by rotation of the

(12) Grill, V.; Shen, J.; Evans, C.; Cooks, R. G. *Rev. Sci. Instrum.* **2001**, *72*, 3149−3179.
(13) Dongre, A. R.; Somogyi, A.; Wysocki, V. H. *J. Mass Spectrom.* **1996**, *31*, 339−350.
(14) Stone, E.; Gillig, E.; Ruotolo, B.; Fuhrer, K.; Gonin, M.; Schultz, A.; Russell, D. H. *Anal. Chem.* **2001**, 73, 2233.
(15) Castoro, J. A.; Nuwaysir, L. M.; Ijames, C. F.; Wilkins, C. L. *Anal. Chem.* **1992**, *64*, 2238.
(16) Chorush, R. A.; Little, D. P.; Beu, S. C.; Wood, T. D.; McLafferty, F. W. *Anal. Chem.* **1995**, *67*, 1042−1046.
(17) Zhong, W. Q.; Nikolaev, E. N.; Futrell, J. H.; Wysocki, V. H. *Anal. Chem.* **1997**, *69*, 2496−2503.
(18) Rakov, V. S.; Futrell, J. H.; Denisov, E. V.; Nikolaev, E. N. *Eur. Mass Spectrom.* **2000**, *6*, 299−317.
(19) Laskin, J.; Futrell, J. H. *Mass Spectrom. Rev.* **2003**, *22*, 158.
(20) Laskin, J.; Denisov, E.; Futrell, J. H. *J. Phys. Chem. B* **2001**, 105, 1895.
(21) Laskin, J.; Denisov, E.; Futrell, J. H. *J. Am. Chem. Soc.* **2000**, 122, 9703.
(22) Laskin, J.; Bailey, T. H.; Futrell, J. H. *J. Am. Chem. Soc.* **2003**, *125*, 1625.
(23) Laskin, J.; Futrell, J. H. *J. Chem. Phys.* **2003**, *119*, 3413.
(24) Baykut, G.; Jertz, R.; Witt, M. *Rapid Commun. Mass Spectrom.* **2000**, *14*, 1238.
(25) O'Connor, P. B.; Costello, C. E. *Rapid Commun. Mass Spectrom.* **2001**, *15*, 1862.
(26) O'Connor, P. B.; Mirgorodskaya, E.; Costello, C. E. *J. Am. Soc. Mass Spectrom.* **2002**, *13*, 402.
(27) Laskin, J.; Denisov, E. V.; Shukla, A. K.; Barlow, S. E.; Futrell, J. H. *Anal. Chem.* **2002**, *74*, 3255.

sample holder. The sample plate and the CQ are located inside a 6-in. cube evacuated by a model E2M40 (14 L/s) mechanical pump (BOC Edwards, Crawley, U.K.). The CQ is a 280 mm long (rod diameter 9.525 mm) operated in the rf-only mode at a static pressure of 10−50 mTorr maintained by leaking the air into the chamber through a leak valve.

Light from a nitrogen laser (337.1 nm, Laser Science Inc, Franklin, MA) is transferred through a 2-m fiber cable (Thermo Oriel, Stratford, CT) and refocused on the target (0.2−0.4-mm spot) using two 75-mm planoconvex lenses. The laser beam is introduced into the vacuum system through a large view window, passes between the CQ rods, and hits the target at 45°. Laser intensity measured using a joulemeter (model J8LP-030, Molectron Detector inc, Portland, OR) is 250 μJ/pulse at the output of the laser and 150 μJ/pulse on the output of the fiber cable. Optimal ion signal was obtained using a tightly focused 30 μJ/pulse laser spot on the target.

Mass-resolving and accumulation quadrupoles (RQ and AQ) are located in a vacuum chamber separated from CQ by a 1-mm hole. This chamber is evacuated by a 350 L/s turbomolecular pump (TMP/NT-360, Leybold, Cologne, Germany) to 5×10^{-5} Torr. Ions are mass-selected by a commercial Extrel quadrupole (200-mm-long, 9.525-mm rod diameter) controlled by a 300-W, 880-kHz 150-QC Extrel power supply (Extrel, Pittsburgh, PA). The RQ has a mass range up to 4000 amu. A collimating plate follows the resolving quadrupole.

The third quadrupole (45-mm-long, 9.525-mm rod diameter) used for ion accumulation and collisional relaxation of mass-selected ions is enclosed in a vacuum-sealed container pumped through two 1-mm appertures in the trapping plates. The pressure in AQ is maintained by leaking collision gas through a 300-mm-long tube (2-mm i.d.) with a backing pressure monitored by a thermocouple gauge. The pressure in the accumulation quadrupole can be varied between 1×10^{-4} and 2×10^{-3} Torr without significantly affecting the pressure in the rest of the vacuum system. Both collisional and accumulation quadrupoles are powered by a PNNL-built high-Q head operated at a frequency of ~850 kHz and the peak-to-peak voltage of 600−700 V. Ions from one or several laser pulses are accumulated in the AQ and extracted into the ICR cell. The AQ is short enough so that ions extracted from the AQ have a very well-defined and fairly narrow (<2 eV fwhm) distribution of kinetic energies,[27] important for effective trapping in the ICR cell. Typical MALDI interface voltages are as follows: sample plate voltage, 30−40 V; CQ offset, 25 V; conductance limit, 10−12 V; RQ offset, 7 V; AQ offset, 4−6 V. AQ front and back trapping plates are kept at +14 and +17 V, respectively, during ion accumulation and relaxation, and +30 and −10 V, respectively, during extraction of ions from the quadrupole.

In the MS mode, ions are transferred into the ICR cell using an electrostatic ion guide[27] and trapped using gated trapping. Trapping conditions are optimized by floating the entire ICR cell off the ground potential and adjusting the time-of-flight delay. MS/MS is achieved by colliding externally produced ions with a surface introduced to the rear trapping plate of the ICR cell using a custom probe and vacuum-lock system. An important feature of our experimental approach is that the kinetic energy of the ions striking the surface is varied by changing the dc offset applied to the ICR cell. The collision energy is defined by the difference

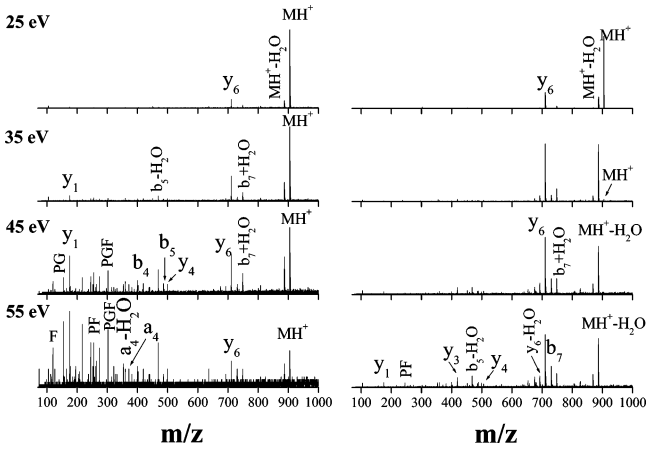

Figure 2. SID (left) and SORI-CID (right) spectra of des-Arg[1]-bradykinin (PPGFSPFR). The amount of dissociation in SORI-CID spectra is varied by changing the peak-to-peak excitation voltage from the value resulting in little fragmentation (top panel) to the maximum value, at which the ion loss became significant (>50%) (bottom panel).

in the potential applied to the accumulation quadrupole and the potential applied to the rear trapping plate and the SID target. The ICR cell can be offset above or below ground by as much as ±150 V. Lowering the ICR cell below ground while keeping the potential on the third quadrupole fixed increases collision energy for positive ions. Because the translational energy of the ion is changed within the constant high magnetic field region of the ICR, ion transmission characteristics of the instrument remain the same at all collision energies. Consequently, parent ion currents and ion trajectories are constant and independent of collision energy.[27] Firing of the laser, ion trapping in the AQ, and voltages on the ICR cell along with ion excitation and detection are controlled by a Midas data station.[28]

All peptides were purchased from Sigma (St. Louis, MO) and used without further purification. MALDI samples were prepared using the dried-droplet method with 2,5-dihydroxybenzoic acid (DHB) as a matrix. Peptide solutions (10−20 μM in 0.1% TFA in water) were premixed with 20 mg/mL DHB in methanol, and 0.5−1 μL of the resulting solution was deposited onto the sample plate.

The SID surface used in this study is a 2-μm-thick film of carbon vapor-deposited diamond on titanium disk prepared by P1 Diamond Inc. (Santa Clara, CA).

RESULTS AND DISCUSSION

Figures 2 and 3 compare SORI-CID (right panel) and SID (left panel) fragmentation spectra of singly protonated des-Arg[1]-bradykinin and renin substrate tetradecapeptide (porcine-DRVYIHPFHLLVYS), respectively, generated by MALDI. SID spectra were obtained by collecting mass-selected ions of interest from five laser shots in the accumulation quadrupole prior to extraction into the ICR cell. Each spectrum represents an average of 10 acquisitions corresponding to an average over 50 laser shots. In all cases, the spectra are ordered from the low-energy collisions at the top to high-energy collisions at the bottom. SID collision energies were chosen for each peptide in such a way that minimal

(28) Senko, M. W.; Canterbury, J. D.; Guan, S.; Marshall, A. G. *Rapid Commun. Mass Spectrom.* **1996**, *10*, 1839.

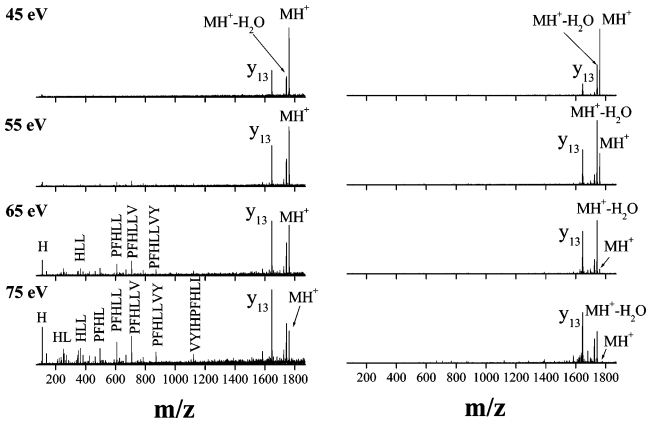

Figure 3. Same as Figure 2 for renin substrate tetradecapeptide porcine (DRVYIHPFHLLVYS).

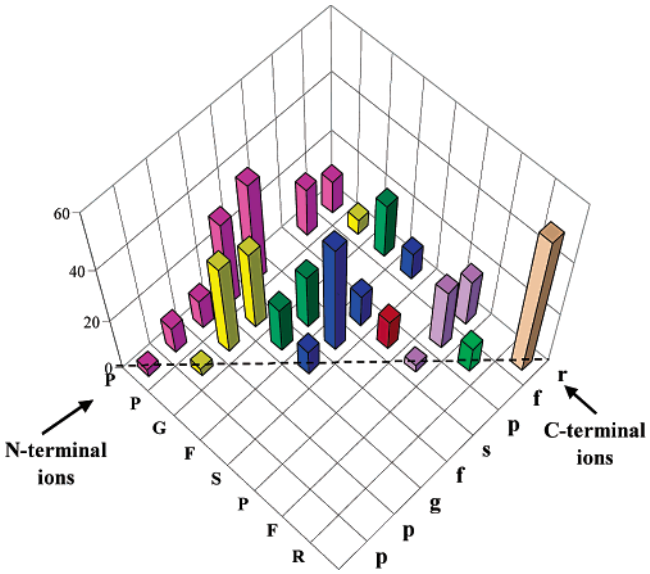

Figure 4. Backbone fragmentation map for the 55-eV SID of des-Arg[1]-bradykinin. The capital letters denote the N-terminal amino acid residue in the fragment ion sequence, and the lowercase letters correspond to the C-terminal amino acid residue (see text for a more detailed discussion).

fragmentation was observed at the lowest energy and extensive fragmentation observed at the highest collision energy. For SORI-CID the peak-to-peak excitation voltage did not exceed the value beyond which ion loss became significant (>50%). We found that in all cases further increase in the SORI excitation voltage did not result in appearance of additional fragment ions while overall signal intensity decreased dramatically.

At low collision energies, des-Arg[1]-bradykinin undergoes very specific fragmentation (Figure 2) corresponding to the loss of water and cleavage of one backbone bond forming the y_6 fragment. Low-energy SORI-CID and SID spectra are very similar. At higher SORI-CID amplitudes the new fragmentation channel forming the $b_7 + H_2O$ ion, characteristic of the C-terminal arginine residue,[29] is observed. In addition, multiple losses of small molecules from both the precursor ion and its primary fragments are present in SORI-CID spectra. It should be noted that the precursor ion is completely fragmented at all SORI amplitudes except for the lowest one. Only at the highest excitation amplitude are small intensities of lower-mass fragments observed in the SORI-CID spectrum. However, high-energy SID spectra are markedly different from SORI-CID spectra. At 45 eV collision energy a large number of backbone fragment ions are formed by SID, while a substantial fraction of precursor ions remains intact. The relative abundance of fragment ions is further increased by increasing the collision energy to 55 eV. Note that even at this collision energy some precursor ions are present in the spectrum. As mentioned earlier opening of a large number of dissociation channels occurs at higher SID collision energies as a result of shattering of ions on the surface. Further, because of a wide internal energy distribution deposited into ions by collisions with a stiff surface there is an efficient mixing of slow and fast fragmentation pathways, resulting in good sequence coverage. Fragmentation patterns obtained for des-Arg[1]-bradykinin using soft and stiff surfaces have been presented elsewhere.[30] In contrast to SID, SORI-CID spectra are dominated by slow dissociation pathways offering significantly less informative fragmentation.

Because the rate of statistical (slow) fragmentation decreases rapidly with increase in the size of the ion, it is expected that obtaining good fragmentation patterns for larger ions using SORI-CID is even more challenging. This is illustrated in Figure 3 showing fragmentation spectra for a singly protonated 14-residue peptide (DRVYIHPFHLLVYS). SORI-CID spectra contain only fragment ions corresponding to multiple water losses from the precursor ion and the $\mathbf{y_{13}}$ fragment formed by selective cleavage C-terminal to the aspartic acid residue (D).[31−34] The only conclusion that can be reached using such fragmentation pattern for a peptide with unknown sequence is that it contains an N-terminal aspartic acid residue. Similar to the case of des-Arg[1]-bradykinin, low-energy SID spectra closely resemble SORI-CID spectra. However, at higher collision energies (65 and 75 eV), a large number of sequence-specific fragment ions is formed by ion-surface collisions.

Figures 4 and 5 show detailed maps of fragment ions observed in high-energy SID spectra of des-Arg[1]-bradykinin (PPGFSPFR) and renin substrate tetradecapeptide (DRVYIHPFHLLVYS). In these figures, *x*- and *y*-axes correspond to the first (N-terminal) and the last (C-terminal) amino acid residues, respectively, in the sequence of a particular peptide fragment while the *z*-axis corresponds to peak intensities. N-Terminal residues are labeled using capital letters, while C-terminal residues are labeled using lower case letters. For example, in Figure 4, all fragment ions that begin with the phenylalanine residue (F) are shown as dark blue bars with the first bar located at the crossover of the **F** and **f** rows. This corresponds to the immonium ion of phenylalanine. The second (most intense) bar in the same row located at the crossover of the **F** and **s** rows corresponds to the FS internal fragment, the third bar corresponds to the FSP fragment, while the last bar located at the crossover of the **F** and **r** rows

(29) Thorne, G. C.; Ballard, K. D.; Gaskell, S. J. *J. Am. Soc. Mass Spectrom.* **1990**, *1*, 249.
(30) Laskin, J.; Futrell, J. H. *Mass Spectrom. Rev.*, submitted.
(31) Yu, W.; Vath, J. E.; Huberty, M. C.; Martin, S. A. *Anal. Chem.* **1993**, *65*, 3015−3023.
(32) Qin, J.; Chait, B. T. *J. Am. Chem. Soc.* **1995**, *117*, 5411−5412.
(33) Summerfield, S. G.; Whiting, A.; Gaskell, S. J. *Int. J. Mass Spectrom. Ion Processes* **1997**, *162*, 149−161.
(34) Tsaprailis, G.; Somogyi, A.; Nikolaev, E. N.; Wysocki, V. H. *Int. J. Mass Spectrom.* **2000**, *195/196*, 467−479.

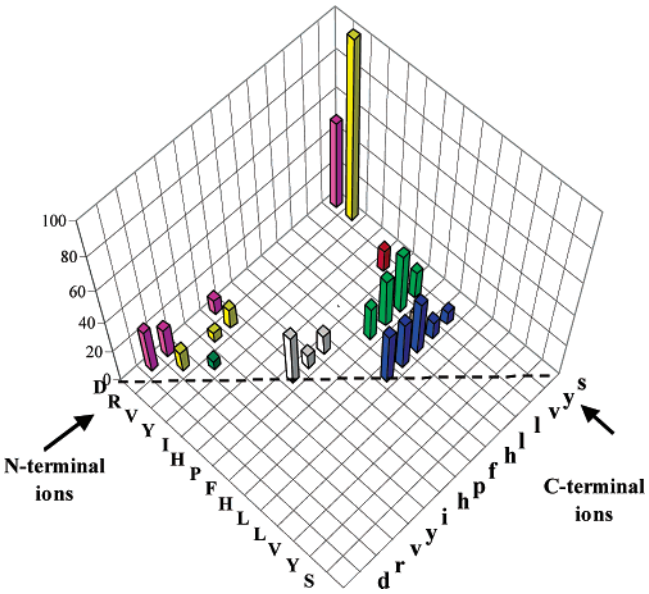

Figure 5. Same as Figure 4 for the 75-eV SID of renin substrate tetradecapeptide porcine (DRVYIHPFHLLVYS).

corresponds to the y_5 fragment ion. Similarly, the yellow bars represent the immonium ion of proline (P), the PG and PGF internal fragments and the y_7 fragment located at the crossover of the second **P** and **r** rows. The dashed line along one of the diagonals of the *XY* plane shows the expected position of immonium ions. The arrows highlight the rows containing the C-terminal and N-terminal ions.

Several additional notes are necessary to clarify the information content of Figures 4 and 5. The bars located in the corners along the dashed line represent combined abundance of the b_1 or y_1 fragment ions and the corresponding immonium ions. For example, the bar located at the crossover of the **R** and **r** rows in Figure 4 represents the combined intensity of the y_1 and R ions. Because the b_1 ion was not observed in the SID spectrum, the bar in the opposite corner represents only the normalized abundance of the proline immonium ion (P). A similar approach was used to represent normalized abundances of other fragment ions that formally correspond to the same sequence. For example, the intensities of the b_4, a_4, and a_4-18 ions are added together to represent the overall abundance of the PPGF sequence in the spectrum. Finally, the bar in the corner of Figure 4 located at the crossover of the first **P** and **r** rows represents the combined abundance of fragment ions corresponding to loss of small molecules from the precursor ion.

This graphic representation of the information content of SID spectra allows us to summarize all backbone fragments, usually accounting for more than 90% of the overall SID fragmentation, in one chart. It is clear from Figure 4 that high-energy SID of des-Arg[1]-bradykinin results in an almost complete series of sequence-specific N-terminal fragments (mainly b_n and b_n-NH_3 ions), a good series of y ions, and a large number of internal fragments mainly consisting of 2−3 amino acid residues. At the same time, the intact precursor ion is present in the spectrum, highly advantageous for peptide identification. The major fragment of renin substrate tetradecapeptide (Figure 5) corresponds to the selective cleavage C-terminal to the aspartic acid resulting in formation of the y_{13} fragment. However, in contrast to SORI-CID

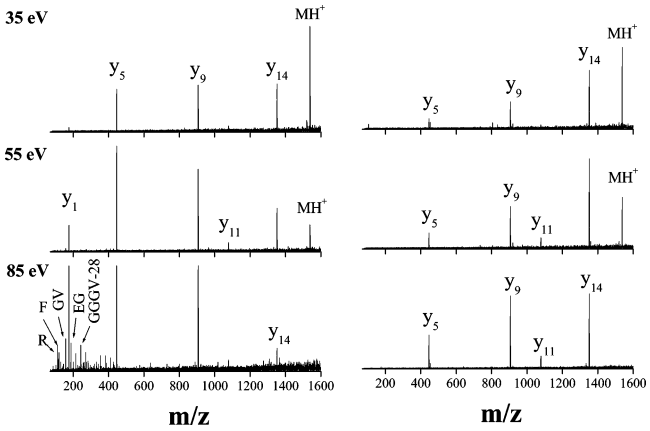

Figure 6. Same as Figure 2 for fibrinopeptide A (ADSGEGDFLAE-GGGVR).

(Figure 3, right panel), for which the y_{13} is the only sequence-specific fragment, high-energy SID produces several small b ions and a very informative series of internal fragments with arginine, proline, and both histidine residues at the N-terminus.

The last example we have examined, which was the least successful case in terms of the information contents of high-energy SID spectra, is shown in Figure 6. Fragmentation of fibrinopeptide A (ADSGEGDFLAEGGGVR) is dominated by y ions corresponding to selective cleavages at two aspartic and two glutamic acid residues. These are the only fragments observed using SORI-CID. High-energy SID results in formation of a large number of low-intensity low-mass fragments (m/z <450). No additional high-mass fragments are obtained using SID. This information can be potentially useful for peptide sequencing using the recently proposed patchwork approach[35] that utilizes accurate mass measurement of low-mass fragments including internal fragments for peptide identification. Further discussion of this topic is beyond the scope of this paper. Work in progress in our laboratory in collaboration with Wysocki group from the University of Arizona will address this question in detail.

CONCLUSIONS

First results on surface-induced dissociation of MALDI-generated ions in FT-ICR MS demonstrated unique advantages of SID over SORI-CID for structural characterization of singly protonated peptide ions. As expected based on our prior experience,[19,20] both slow activation by gas-phase collisions (SORI-CID) and fast excitation of ions by collisions with surfaces at relatively low collision energies provide similar fragmentation patterns. However, at higher collision energies, SID fragmentation of peptide ions is dominated by shattering,[22] resulting in formation of a large number of sequence-specific fragment ions. Although the transition from recoil (slow decay) to shattering (fast decay) is a fairly sharp function of the internal energy of the ion, ion−surface impact results in deposition of a distribution of internal energies into the ensemble of ions that effectively mixes the slow and fast decay in the resulting SID spectrum. In this work, we took additional advantage of a wide internal energy distribution of ions resulting from collision with a stiff diamond surface that provides a better mixing of slow and fast fragmentation channels.

(35) Schlosser, A.; Lehmann, W. D. *Proteomics* **2002**, *2*, 524.

We have specifically demonstrated that SID results in a significantly better sequence coverage for singly protonated ions that are difficult to fragment using conventional ion activation techniques in FT-ICR MS. It follows that combination of SID with MALDI FT-ICR MS is a new powerful method for characterization and identification of biomolecules.

ACKNOWLEDGMENT

This work was conducted at the W. R. Wiley Environmental Molecular Sciences Laboratory (EMSL), a national scientific user facility sponsored by the U.S. Department of Energy and located at Pacific Northwest National Laboratory. PNNL is operated by Battelle for the U.S. Department of Energy. Research at EMSL was carried out within the project 40457 supported by the Office of Basic Energy Sciences of the U.S. Department of Energy. J.J.H. was supported by an ERULF fellowship, which is gratefully acknowledged. The authors are gratefully thankful to Ekaterina Mirgorodskaya, Peter O'Connor, Gökhan Baykut, Mattias Witt, and Franz Hillenkamp for helpful discussions on various aspects of MALDI FT-ICR experiments. We also thank John Wronka for providing us with a sample probe assembly for the MALDI source.

Received for review September 22, 2003. Accepted October 31, 2003.

AC0351116